Manuscript

Strong substrate mediation of attractive lateral interactions of CO on Cu(110)

José A. Garrido Torres[‡], Kirsten L. Finley[‡], Herbert A. Früchtl, Paul B. Webb[*], Renald Schaub[*]

EaStCHEM and School of Chemistry, University of St Andrews, KY16 9ST, St Andrews, UK

Corresponding Authors: * RS: renald.schaub@st-andrews.ac.uk; PBW: pbw@st-andrews.ac.uk

Author Contributions: ‡ These authors contributed equally.

Supplementary Information (SI) available: [details here].

Abstract

The mechanism of chemical reactions between adsorbed species is defined by the combined effects of the adsorbate-substrate potential landscape and lateral interactions. Such lateral interactions are therefore integral to catalytic processes, but their study is often complicated by 'substrate mediation', the regulation of a two-body potential between adsorbed particles by the surface itself. Substrate mediation can influence the sign and magnitude of lateral interactions. There are notable exceptions of ordered structures forming at low coverage, indicative of short range attractive forces where repulsive forces are expected to dominate, suggesting a strong substrate mediated contribution. To explore further the origins of such interactions we have investigated the adsorption of CO on Cu(110) using a combination of low temperature microscopy and first principles calculations. Our studies reveal that lateral adsorbate interactions, which are constrained by the metal surface, regulate the bonding between adsorbate and substrate. Anisotropic CO–CO coupling is seen to arise from a perfect balance between the intermolecular accumulation of charge that acts as a glue (chemical coupling) at sufficiently large distances to avoid repulsive effects (dipole-dipole coupling and Pauli repulsion between electron clouds).

Introduction

An ability to deliberately construct every element of a catalyst's structure would revolutionise catalyst design. To achieve this ambitious goal we must first identify the nature of sites responsible for catalytic activity and develop an understanding of how a catalyst operates at an atomic level. Identifying such structure-function relationships is an arduous task owing largely to the complexity of heterogeneous materials. Attempts to unravel relationships between structure and catalytic response are then often hindered by the necessity to accurately describe the arrangement of contiguous atoms comprising active centres under operating conditions, one of the great challenges in heterogeneous catalysis. The problem is complicated further by the effects of adsorbate lateral interactions, which play a significant role in defining the adsorbate distribution functions that influence a broad range of surface phenomena including ensemble effects in catalysis.[1]

The combination of adsorbate-substrate potential and lateral interactions determines the mechanism and activation parameters of chemical reactions between adsorbed species. The study of such interactions is therefore integral to the understanding of catalytic processes[2-4] but is far from trivial owing principally to 'substrate mediation', an often and loosely used term, which alludes to the modification of a two-body potential between adsorbed particles by the surface itself.[1] Substrate mediation can influence the sign and magnitude of lateral interactions, but despite its importance, substrate mediation is a poorly understood phenomenon.

From a catalysis perspective, carbon monoxide is the archetypal probe of surface structure; it is a reactant in numerous chemical processes and its bonding strength (as deduced from vibrational spectroscopy) is sensitive to the local environment[5], intimately dependent on the nature of the CO-metal interaction and the local coverage (intermolecular interaction). At low coverages the repulsive nature of intermolecular interactions prevents the formation of ordered CO structures. Beyond nearest neighbor distances, CO-CO interactions become non-monotonic as a function of coverage with ordered overlayers forming, via close packing, at sufficiently high coverages. Several models describing the interaction of CO with noble metals have been developed and differ largely in how the balance between σ and π interactions is considered.[6-13]

There is a notable exception to this general behavior; using STM Briner *et al.*[14] observed the CO–CO interactions on a Cu(110) surface to be highly anisotropic. Along the $[1\bar{1}0]$ surface direction interactions are repulsive but are, very surprisingly, attractive at nearest neighbor distances along the [001] surface

direction allowing ordered structures to form even at low coverages. The authors hypothesized that this unusual behavior results from 'substrate mediation' but no further explanation was provided to rationalize the origin of such substrate effects.

To investigate further the intermolecular interactions between adsorbed CO at low coverage, and the potential impact on the nature of adsorbate-substrate bonding, we have examined CO adsorption on Cu(110) using atom-resolved Scanning Tunneling Microscopy (STM) and first principles calculations based on Density Functional Theory (DFT). The STM approach allows for a direct assessment of surface structure and its influence on the interplay between dynamic coupling in the adlayer and adsorbate-substrate interactions. While previous work on this system has focused predominantly on higher CO coverages,[15-18] we have explored the low-coverage regime (~0.06 monolayers) to facilitate investigation of the individual components of the CO–CO and CO–Cu interaction in detail. In accordance with work published by Briner *et al.*[14] we too have observed the formation of linear CO chains oriented exclusively in the [001] direction of the substrate. This uncharacteristic and highly anisotropic CO intermolecular interaction is shown, through a combination of experimental and theoretical findings, to arise from a substrate-mediated intermolecular charge accumulation. As a consequence, the typical intermolecular repulsion is negated at CO-CO distances that are sufficiently large.

Results and discussion

Figs. 1a,b show high-resolution STM images acquired at approximately 4 K, after dosing the Cu(110) with ~0.05 L CO at 150 K, yielding a surface coverage of 0.06 ML CO. Well-resolved images were reproducibly acquired when scanning at a bias voltage (V_t) of approx. ±0.1 V and a tunneling current (I_t) of ~1 nA. These images closely resemble those reported by Briner *et al*.[14] In all scanned areas, we observe circular features together with linear chains composed of discrete lengths and strictly aligned with the [001] direction, perpendicular to the close-packed Cu rows. The small circular-shaped depressions have dimensions expected for isolated CO molecules (monomers). We therefore assign the chain-like features, consisting of dark depressions separated by bright circular-shaped areas, to molecular arrangements of CO positioned at nearest neighbor sites along the [001] direction, and refer to these arrangements as *n*-mers composed of *n* CO molecules. Dimers, which are the simplest arrangement generated by intermolecular interactions, possess one central bright feature. Subsequently, *n*-1 bright features are

expected to appear within an *n*-meric chain. The origin of these bright features will be the focus of our discussions below. Superimposing a (110) lattice grid, as shown in **Fig. 1b**, reveals that all CO molecules (monomers and constituents of *n*-mers) are adsorbed on equivalent surface sites. These CO adsorption sites are identified theoretically (see below) as on-top copper sites.

Several aspects of the CO/Cu(110) system are remarkable. Firstly, monomer diffusion is expected to be significantly favored along the close-packed $[1\bar{1}0]$ direction, whilst the chain growth direction is perpendicular to it ([001] direction). Secondly, the formation of strictly one-dimensional CO clusters implies a strong anisotropy in CO–CO lateral interactions: these seem to be attractive and repulsive at nearest neighbor distances along the [001] and $[1\bar{1}0]$ directions respectively. We have never observed two CO monomers or *n*-mers at nearest neighbor sites along the $[1\bar{1}0]$ direction. Thirdly, when two CO molecules are adjacent in the [001] direction, an additional protrusion is visible in between the molecules. This protrusion must have an electronic origin resulting from the intermolecular interaction. Moreover, it is likely mediated by the metal support (as we will demonstrate below) and hence holds the clue to understanding the nature of the uncharacteristic anisotropic CO–CO bonding mechanism. In what follows, we address these three aspects.

Our CO deposition experiments are conducted on the copper substrate held at 150 K. At this temperature CO is sufficiently mobile to achieve equilibrium on the surface prior to measurements (note that STM data acquisition is carried out at ~4 K and as such thermal diffusion of CO on the surface can be ruled out during measurements). Indeed, the observed exponential decay of the number of clusters as a function of CO content (**Fig. 1c**) confirms thermal equilibration. We expect this to be reached mainly through a process of unidirectional CO diffusion along the $[1\bar{1}0]$ direction. If this hypothesis is correct, a higher density of adsorbates trapped at step edges aligned perpendicular to the direction of diffusion would be expected (this also assumes the step edges to act as trapping centers for CO molecules, as is the case for many similar systems[19,20]). This is indeed the case; STM images (**Fig. 2**) clearly show a significant, preferential decoration of the [001] step edges as compared to the $[1\bar{1}0]$ steps. For the latter, the number of trapped CO molecules correlates to the density of deposited CO, whereas for the former, decoration is almost complete.

Further experimental evidence for unidirectional diffusion comes from manipulation experiments[21] whereby the STM tip is used to induce lateral movement of individual CO molecules on the surface. It was found that the CO molecules could only be displaced by one or two adsorption sites in the $[1\bar{1}0]$ direction along the Cu rows, in the opposite direction to the movement of the STM tip. **Fig. 1d** shows

consecutive STM images following lateral displacements of a single CO molecule along the [$1\bar{1}0$] direction (manipulation parameters are reported in the **SI**). The first displacement procedure (direction indicated by the red arrow in **Fig. 1d**) caused the CO molecule to move one adsorption site along the [$1\bar{1}0$] direction. A Cu(110) lattice grid has been superimposed to show clearly the displacement of the CO molecule towards a CO dimer. The second manipulation procedure resulted in the CO molecule moving by two adsorption sites to form a trimer. We note here that all attempts to: (1) induce a displacement perpendicular to the [$1\bar{1}0$] direction and, (2) bring two CO molecules at nearest neighbor distance along the [$1\bar{1}0$] direction, were unsuccessful.

Following these molecular manipulations, the area shown in **Fig. 1d** was scanned at a lower tunneling gap for increased resolution, and the result is shown in **Fig. 1b**. The two highlighted trimers are well resolved and are identical in appearance: one was formed during sample preparation, and the other was formed as a result of controlled lateral manipulations. This proves our earlier assignment on the origin of the molecular chains as resulting from the formation of linear CO aggregates, with *n*-meric chains exhibiting *n*-1 bright features.

To provide greater insight into the anisotropic CO–CO interaction on the Cu(110) surface, we revert to DFT calculations. Computed adsorption energies for the monomer on Cu(110) reveal that the on-top site (**Fig. 3a**) is 63 meV more stable than the two-fold short-bridge site – the second most stable adsorption site (see **SI**). Dimers arranged in the [001] direction (**Fig. 3a**) show a marked increase in stability for both on-top and short-bridge adsorption sites when compared to their respective monomers. Geometry optimizations for each CO pair were also performed and are shown in **Fig. 3b** adsorbed at different relative positions along both the [001] and [$1\bar{1}0$] high-symmetry directions of the substrate. The resulting adsorption energies for these arrangements are shown in **Fig. 3c**. The preferred relative coordination, labelled as L1, corresponds to the CO pair adsorbed at nearest neighbor on-top sites in the [001] direction (as shown in **Fig. 3a** top-right). When comparing the adsorption energy per CO molecule, this L1 arrangement is found to be more stable than the preferred adsorption geometry for CO monomers (energy indicated by the horizontal red dashed line in **Fig. 3c**). This is not the case for any other arrangement. The formation of unidirectional CO chains is further confirmed by considering a system containing three CO molecules at different relative positions (**Fig. 4a**: dimer + monomer, and **Fig. 4b**: trimer). The system with the lower nearest-neighbor intermolecular coordination is 18 meV less stable than the more highly coordinated system. From this we conclude that the addition of a monomer to an *n*-

mer along the [001] direction is an energetically favorable process that provides the driving force for the growth of linear CO aggregates at our experimental conditions of deposition (150 K).

The simulated STM images for the corresponding optimized structures are shown at the bottom of **Figs. 4a,b**. In the first case, one can recognize the well-known "sombrero shape" of the isolated CO monomer[22], whilst the dimer exhibits an increased brightness in the intermolecular region shared between the two CO molecules. In the second case, the trimer exhibits two areas of increased brightness located in between pairs of CO molecules. Hence, the simulated STM images replicate the experimental images very accurately, reproducing the observed small circular features assigned to the monomers and the *n*-1 regions of increased electronic contrast between the *n*-mer constituents.

To assess the anisotropic CO diffusion, NEB calculations (see **SI**) were performed to probe for the movement of a CO molecule from an on-top site to the adjacent on-top site for both [001] and $[1\bar{1}0]$ directions. We found a substantially preferred movement along the $[1\bar{1}0]$ high-symmetry direction, as expected, for which the CO molecule has to overcome a diffusion barrier of 70 meV. In contrast, there is a significantly higher energy barrier (> 400 meV) to diffusion along the [001] direction, or when following a translation coordinate which combines both directions (> 500 meV).

By combining our microscopic observations and theoretical calculations, the following mechanism for the formation of linear CO aggregates emerges. Under our deposition conditions (the Cu(110) sample being kept at 150 K), CO molecules undergo diffusion strictly along the $[1\bar{1}0]$ direction, from on-top to on-top sites. Two CO molecules will dimerise only if their respective unidirectional diffusion brings them to nearest-neighbor distance along the [001] direction. Further *n*-mer growth, restricted to the [001] direction, can subsequently (and solely) proceed by capture/stabilization of diffusing monomers at the chain ends.

We now turn to the question of the origin of the bright features, observed both experimentally (**Fig. 1**) and theoretically (**Fig. 4**) between CO molecules constituting the linear aggregates, and what these might reveal about the anisotropic intermolecular bonding mechanism. To investigate this, in **Fig. 5a** we compare adsorption induced charge difference density plots for two systems: two isolated monomers and their resulting dimer. The plots show an iso-surface of $5 \cdot 10^{-4}$ electrons/Å in the density difference. This value was chosen to maximize contrast; other values show qualitatively the same picture. The two systems shown consist of a pair of CO molecules arranged along the two high-symmetry directions of the substrate, the favorable [001] and the unfavorable $[1\bar{1}0]$ directions. The areas denoted in red and blue indicate the

accumulation and depletion of electronic charge, respectively. In the case of the monomers approaching along the [001] direction, two regions of depleted charge (the blue features highlighted by the green marquees in **Fig. 5a**) come into contact when dimerizing. Conversely, two regions of accumulated charge (red features) interact when forming a dimer in the $[1\bar{1}0]$ direction. This difference is insufficient to justify the interaction anisotropy. Indeed, an enhancement of electronic charge between the two CO molecules is revealed when constituting the dimers for both alignments (compare in **Fig. 5b** the plane cuts α and α' for the $[1\bar{1}0]$ alignment, and the plane cuts σ and σ' for the [001] alignment). We note here that these charge difference calculations were performed by subtracting the density of dimer in the gas phase (and not the two separate monomers) and the substrate from the combined dimer-substrate system. Hence, the enhanced charge accumulation arises mainly from the coupling of the dimer to the substrate, and not from CO–CO interaction within the dimer. From this, we most importantly conclude that it is a result of the chemical coupling of laterally interacting adsorbates with the metal substrate. We therefore propose that this accumulation of electron density between CO molecules at nearest neighbor sites is the main factor determining intermolecular bonding on the Cu(110) surface. It is also responsible for the bright features observed in both our experimental and theoretical STM images.

Since the accumulation of charge is theoretically predicted for both $[1\bar{1}0]$ and [001] aligned dimers, a second factor needs to be considered, involving geometric constraints imposed by the substrate, to account for the strong directionality of the bonding. The periodicity of the Cu(110) surface, and consequently the nearest neighbor distance for CO monomers, is 2.56 Å and 3.62 Å along the $[1\bar{1}0]$ and [001] directions respectively. In the limit of zero intermolecular interactions, the CO molecular axis is perpendicular to the surface plane (see plane cuts β and τ in **Fig. 5b**). When two monomers couple to form the most energetically favorable dimer (along the [001] direction), their molecular axes remain almost unaltered (plane cut β'). In contrast, the repulsive interaction between the two CO molecules becomes evident from the strong distortion of the molecular axes when forming dimers along the less favorable $[1\bar{1}0]$ direction (plane cut τ' in **Fig. 5b**). In the latter case, the CO molecules are within too close a proximity to overcome this electronic hindrance. Conversely, in the former case the CO–CO distance is such that there is an appropriate balance between the intermolecular accumulation of charge (resulting from chemical coupling) acting as a glue, but at sufficient distance so as to avoid repulsive effects (resulting from dipole-dipole coupling and Pauli repulsion between electron clouds).

Conclusions

Using high-resolution STM and DFT calculations we have examined the mechanism for attachment of CO molecules on a Cu(110) substrate and their lateral interaction. Preferential decoration of the step edges in the [001] direction, and the displacement of laterally manipulated CO molecules exclusively along the $[1\bar{1}0]$ direction, indicate one-dimensional diffusion along the high-symmetry $[1\bar{1}0]$ Cu rows. Experimental evidence for the formation of molecular CO chains, with the propagation axis oriented along the [001] direction of the substrate, is supported theoretically through DFT calculations. The strongly anisotropic intermolecular interaction arises from a fine balance between charge redistribution and CO–CO separation. The accumulation of electron density between neighboring CO molecules is demonstrated to act as a glue by regulating molecular ordering even at low coverage. Mediation by the Cu(110) surface turns an anticipated CO–CO repulsive interaction into an attractive interaction.

Methods

STM experiments:

Experimental data were collected using a low-temperature (4K) scanning tunneling microscope (CreaTec). The system operates under ultrahigh vacuum (UHV) with a base pressure in the 10^{-11} mbar range. The Cu(110) crystal (MaTeck) was cleaned in vacuum by repeated cycles of Ar ion bombardment (1.5 keV, 0.8 µA ions, 7 min at 300 K) and annealing (825 K, 15 min). The sample was exposed to ~0.05 L CO ($5 \cdot 10^{-9}$ mbar, 10 s) at 150 K prior to being transferred into the LHe cooled STM. Microscopy images were acquired in constant current imaging mode.

First principle calculations:

First principle calculations were performed using Density Functional Theory (DFT[23]), employing a plane-wave basis set and using the Generalized Gradient Approximation (GGA[24]), as implemented in the Vienna Ab-initio Simulation Package (VASP[25-26]). The Projector Augmented Wave (PAW[27,28]) method was used to account for the core-valence interactions. Valence electrons were described using plane-waves

considering an expansion on the kinetic energy up to an energy cut-off of 400 eV. We applied the non-local correlation functional vdW-DF proposed by Dion *et al*.[29], which accounts intrinsically for dispersion interactions. For the calculation of the exchange energy contribution, we employed the revPBE functional[30], which avoids the spurious binding effects associated with vdW-DF[31], by providing a more accurate approximation of the exact exchange. Smearing of the electron population around the Fermi energy was allowed following the Methfessel-Paxton method[32], with a smearing width of 0.1 eV. The copper surface was modelled using four layers in the (110) orientation. The two upper layers, representing the surface, were relaxed during the optimization, whilst the other two were kept fixed at the minimum energy bulk positions, in a supercell periodically repeated in the three dimensional space. A vacuum layer of ~18 Å was introduced to avoid spurious interactions between periodic images. Geometry optimizations were carried out using the Γ-point for the integration of the Brillouin zone, which was considered sufficient for the sampling of a unit cell of 26.20 Å × 25.94 Å (10 × 7) used to simulate the molecules at low coverage on the surface. ZPE corrections were not applied due to the large size of the unit cells. Simulated STM images were computed using the Tersoff-Hamann approximation[33,34] at constant current for positive and negative voltages (specified in the main text). The reported values of adsorption energies (E_{ads}) per CO molecule are calculated as follows:

$$E_{ads} = \frac{n \cdot E_{CO,gas\ phase} + E_{Cu(110)} - E_{CO@Cu(110)}}{n} \qquad (1)$$

Here, *n* refers to the number of CO molecules, which allows for a comparison between systems containing a different number of adsorbed molecules. $E_{CO,gas\ phase}$, $E_{Cu(110)}$, and $E_{CO@Cu(110)}$ are the energies for the single molecule of CO in the gas phase, the copper (110) slab and the adsorbed CO on Cu(110) for the case of interest, respectively. Therefore, a more positive adsorption energy value means a higher stability of the system. Activation energy barriers were determined using the Nudged Elastic Band method[35] (NEB). Climbing image NEB was employed to find the minimum energy path between geometries, using modified VASP routines from Henkelmann[36]. We used 14 images for the scan of each barrier reported to obtain the activation energies for the translational mechanism of the CO between different adsorption sites. A Monkhorst-Pack scheme using a denser grid of 3 × 3 × 1 k-points was employed during the NEB calculations to get a high accuracy in the results for the activation barriers, due to the fact that the later simulations were carried out using a smaller 6 × 4 unit cell (15.72 Å × 14.82 Å). All optimizations were carried out using the conjugate gradient method. The convergence criterion for the electronic self-consistent cycle was fixed at 10^{-5} eV and the forces on all relaxed atoms were required to be smaller than 0.02 eV/Å.

Acknowledgements

We acknowledge financial support from the Scottish Funding Council (through EaStCHEM and SRD-Grant HR07003) and from EPSRC (PhD studentship for JAGT, EP/M506631/1). The Royal Society is gratefully acknowledged for the award of an Industry Fellowship to P.B.W. Computational support was provided via the EaStCHEM Research Computing Facility. The research data supporting this publication can be accessed at: http://dx.doi.org/10.17630/1f738fa6-c19c-414c-818b-1ebee3a75217.[37]

References

[1] S. D. Kevan, Interactions between adsorbed molecules. *J. Mol. Catal. A* **131**, 19–30 (1998).

[2] T. Zambelli, J. Wintterlin, J. Trost, G. Ertl, Identification of the "active sites" of a surface-catalyzed reaction. *Science* **273**, 1688–1690 (1996).

[3] H. S. Taylor, A theory of the catalytic surface. *Proc. R. Soc. Lond. A* **108**, 105–111 (1925).

[4] M. Boudart, Catalysis by supported metals. *Adv. Catal.* **20**, 153–166 (1969).

[5] P. Hollins, The influence of surface defects on the infrared spectra of adsorbed species. *Surf. Sci. Rep.* **16**, 53–94 (1992).

[6] R. Ryberg, in *Advances in Chemical Physics: Molecule Surface Interactions*, Vol. 76 (ed. Lawley, K. P.) (John Wiley & Sons, Inc., Hoboken, NJ, USA, 1989).

[7] M. W. Roberts, J. M. Thomas, *Chemical Physics of Solids and Their Surfaces*, Royal Society of Chemistry, Cambridge, 1st edn., 1978, vol. 7.

[8] D. P. Woodruff, B. E. Hayden, K. Prince, A. M. Bradshaw, Dipole coupling and chemical shifts in IRAS of CO adsorbed on Cu(110). *Surf. Sci.* **123**, 397–412 (1982).

[9] P. S. Bagus, W. Muller, The Origin of the Shift in the C-O Vibration of Chemisorbed Co - Cluster Model Studies for Co/Cu(100). *Chemical Physics Letters* **115**, 540–544 (1985).

[10] D. Heskett, E. W. Plummer, R. P. Messmer, Correlation between Anomalous Electronic and Vibrational Properties of Chemisorbed Systems. *J. Vac. Sci. Technol. A* **2**, 1084-1086 (1984).

[11] P. Hollins, J. Pritchard, Intermolecular interactions and the infrared reflection-absorption spectra of chemisorbed carbon monoxide on copper. *ACS Symposium Series* **137**, 51-74 (1980).

[12] W.-L. Yim, T. Klüner, Substrate Mediated Short- and Long-Range Adsorption Patterns of CO on Ag(110). Phys. Rev. Lett. 110, 196101 (2013).

[13] J. Oh, H. Lim, R. Arafune, J. Jung, M. Kawai, Y. Kim, Lateral Hopping of CO on Ag(110) by Multiple Overtone Excitation. Phys. Rev. Lett. 116, 056101 (2016).

[14] B. G. Briner, M. Doering, H.-P. Rust, A. M. Bradshaw, Microscopic molecular diffusion enhanced by adsorbate interactions. *Science* **278**, 257–260 (1997).

[15] K. Horn, M. Hussain, J. Pritchard, *Surf. Sci.* **63**, 244–253 (1977).

[16] C. Harendt, J. Goschnick, W. Hirschwald, *Surf. Sci.* **152–153**, 453–462 (1985).

[17] R. Davis, R. Lindsay, K. G. Purcell, G. Thornton, A. W. Robinson, T. P. Morrison, M. Bowker, P. D. A. Pudney, M. Surman, A NEXAFS study of the orientation of CO on Cu(110). *J. Phys. Condens. Matter* **3**, S297–S302 (1991).

[18] J. Ahner, D. Mocuta, R. D. Ramsier, J. T. Yates Jr., Adsorbate–adsorbate repulsions — the coverage dependence of the adsorption structure of CO on Cu(110) as studied by electron-stimulated desorption ion angular distribution. *J. Chem. Phys.* **105**, 6556–6559 (1996).

[19] H. Ibach, K. Horn, R. Dorn, H. Lüth, *Surf. Sci.* **38**, 433–454 (1973).

[20] S. Kennou, M. Kamaratos, S. Ladas, C. A. Papageorgopoulos, *Surf. Sci.* **216**, 462–471 (1989).

[21] L. Bartels, G. Meyer, K.-H. Rieder, Basic steps of lateral manipulation of single atoms and diatomic clusters with a scanning tunneling microscope tip. *Phys. Rev. Lett.* **79**, 697–700 (1997).

[22] L. Bartels, G. Meyer, K.-H. Rieder, Controlled vertical manipulation of single CO molecules with the scanning tunneling microscope: A route to chemical contrast. *Appl. Phys. Lett.* **71**, 213 (1997).

[23] W. Kohn, L. J. Sham, Self-consistent equations including exchange and correlation effects. *Phys. Rev.* **140**, A1133–A1138 (1965).

[24] J. P. Perdew, K. Burke, M. Ernzerhof, Generalized gradient approximation made simple. *Phys. Rev. Lett.* **77**, 3865–3868 (1996).

[25] G. Kresse, J. Furthmüller, Efficiency of ab-initio total energy calculations for metals and semiconductors using a plane-wave basis set. *Comput. Mater. Sci.* **6**, 15–50 (1996).

[26] G. Kresse, J. Hafner, Ab initio molecular dynamics for liquid metals. *Phys. Rev. B* **47**, 558–561 (1993).

[27] G. Kresse, D. Joubert, From ultrasoft pseudopotentials to the projector augmented-wave method. *Phys. Rev. B* **59**, 1758–1775 (1999).

[28] P. E. Blöchl, Projector augmented-wave method. *Phys. Rev. B* **50**, 17953–17979 (1994).

[29] M. Dion, H. Rydberg, E. Schröder, D. C. Langreth, B. I. Lundqvist, Van der Waals density functional for general geometries. *Phys. Rev. Lett.* **92**, 246401 (2004).

[30] Y. Zhang, W. Yang, Comment on 'generalized gradient approximation made simple'. *Phys. Rev. Lett.* **80**, 890–890 (1998).

[31] P. Lazić, M. Alaei, N. Atodiresei, V. Caciuc, R. Brako, S. Blügel, Density functional theory with nonlocal correlation: A key to the solution of the CO adsorption puzzle. *Phys. Rev. B* **81**, 45401 (2010).

[32] M. Methfessel, A. T. Paxton, High-precision sampling for Brillouin-zone integration in metals. *Phys. Rev. B* **40**, 3616–3621 (1989).

[33] J. Tersoff, D. R. Hamann, Theory and application for the scanning tunneling microscope. *Phys. Rev. Lett*. **50**, 1998 (1983).

[34] J. Tersoff, D. R. Hamann, Theory of the scanning tunneling microscope. *Phys. Rev. B* **31**, 805–813 (1985).

[35] G. Mills, H. Jonsson, G. K. Schenter, Reversible work transition state theory: application to dissociative adsorption of hydrogen. *Surf. Sci.* **324**, 305–337 (1995).

[36] G. Henkelman, B. P. Uberuaga, H. Jónsson, Climbing image nudged elastic band method for finding saddle points and minimum energy paths. *J. Chem. Phys.* **113**, 9901–9904 (2000).

[37] J. A. Garrido Torres, K. L. Finley, H. A. Früchtl, P. B. Webb, R. Schaub. Strong substrate mediation of attractive lateral interactions of CO on Cu(110). Dataset. University of St Andrews Research Portal, 2018. http://dx.doi.org/10.17630/1f738fa6-c19c-414c-818b-1ebee3a75217.

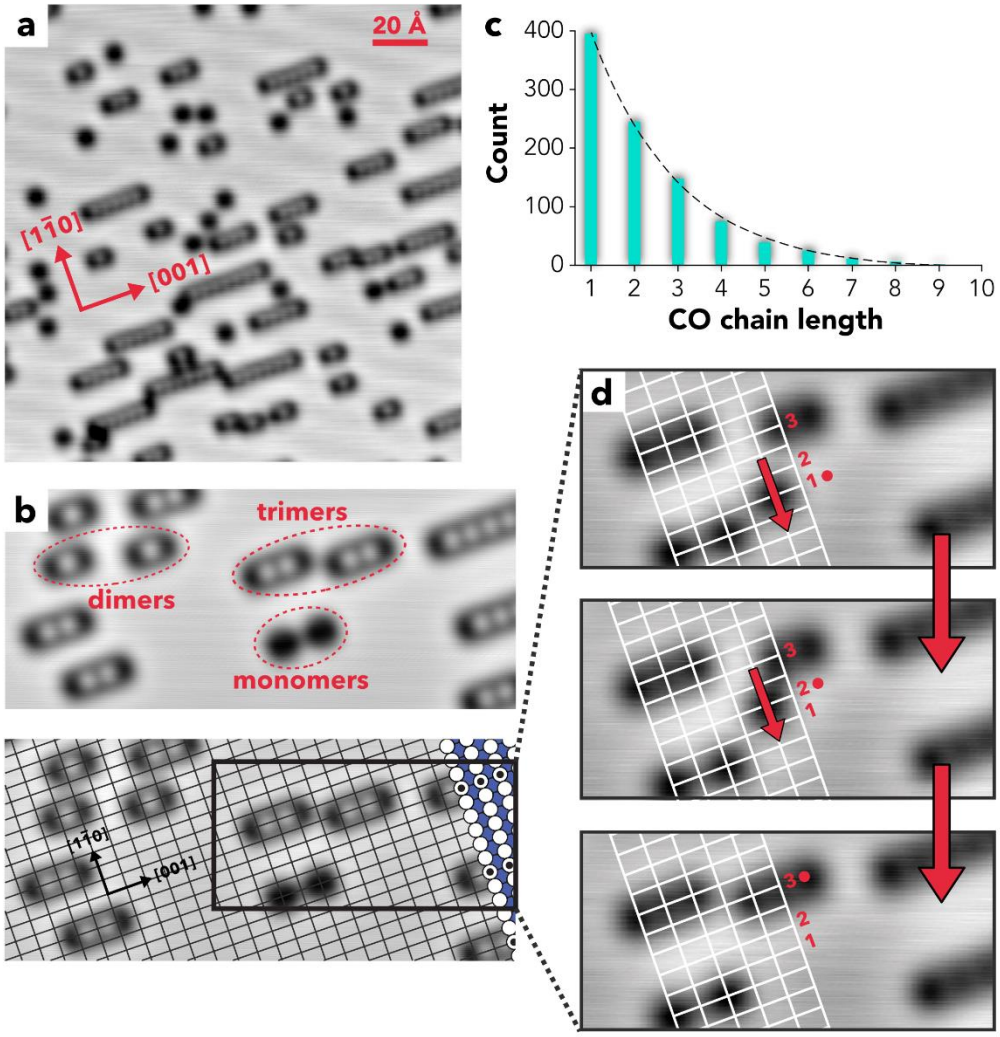

Fig. 1. STM measurements for CO on Cu(110). (a) STM overview of CO on Cu(110) (I_t: 4.0 nA, V_t: 0.10 V). (b) High-resolution STM image exhibiting types of molecular structures observed (I_t: 0.9 nA, V_t: 0.13 V). (c) Counts of the number of CO chains as function of CO content. The dashed line represents an exponential best fit to the data. (d) Sequence of STM images (I_t: 0.05 nA, V_t: 1.04 V) displaying the lateral manipulation of a single CO molecule along the [1$\bar{1}$0] direction. The manipulation direction is opposite to the CO displacement. The CO is brought into nearest-neighbour position of a dimer in order to form a trimer. The resulting image (lower bottom panel of (d)) was then scanned at a lower tunnelling gap, and is shown in (b).

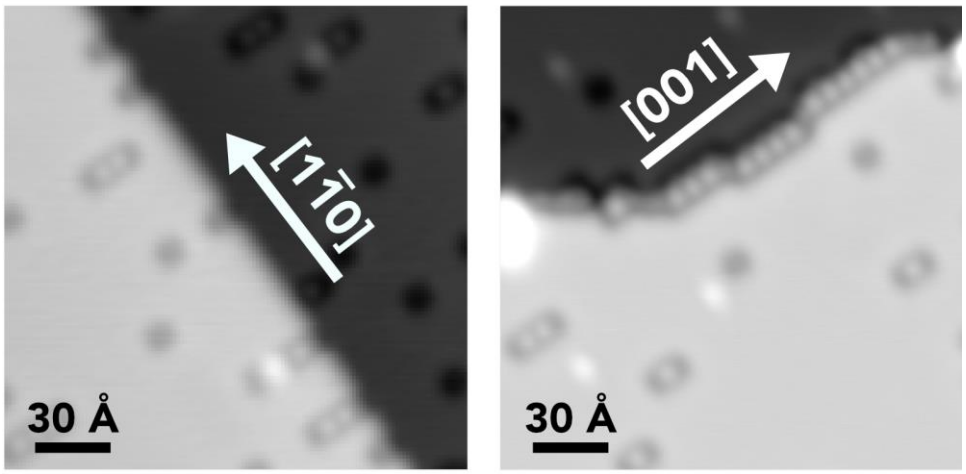

Fig. 2. STM images of two atomic steps on the Cu(110) surface. (I_t: 0.4 nA, V_t: 0.04 V). On the left-hand side, the step edge runs parallel to the [1$\bar{1}$0] direction, whereas on the right-hand side, the step edge runs parallel to the [001] direction, Note the latter step is preferentially decorated with CO molecules.

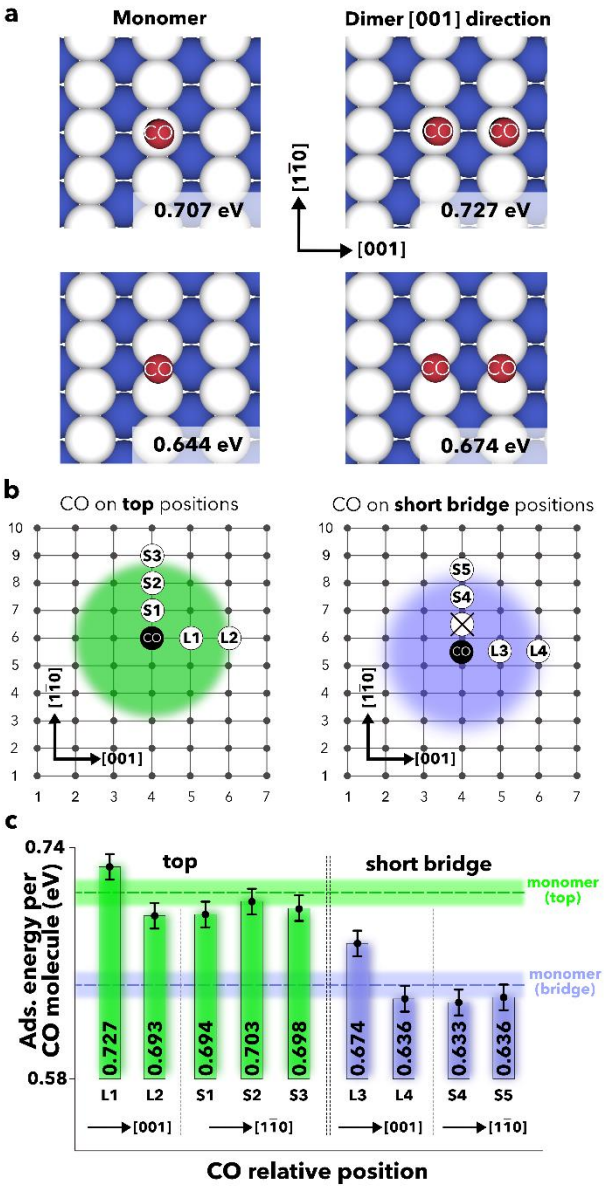

Fig. 3. DFT calculations for CO on Cu(110). (a) Top view of the optimised geometries for monomers (left panels) and dimers (right) adsorbed on top sites (top) and on short-bridge sites (bottom). (b) Schematic representation of the calculated CO pairs located at different relative positions along the [001] and [1$\bar{1}$0] directions for both on-top (left) and short bridge (right) adsorption sites. The CO molecule represented by a black circle serves as a reference. Hence, the labels S1-S5 and L1-L4 indicate the different relative locations of the second CO molecule composing the pair. The L and S labels indicate that the pairs are coordinated following the "long" [001] and "short" [1$\bar{1}$0] directions, respectively. The crossed circle in (b) signifies that, when optimizing at that position, one of the CO molecules forming the dimer relaxed to the nearest pair coordination (S4) due to steric hindrance. (c) Calculated adsorption energies for the CO pairs. The red dashed line represents the adsorption energy for the monomer on the most stable on-top site.

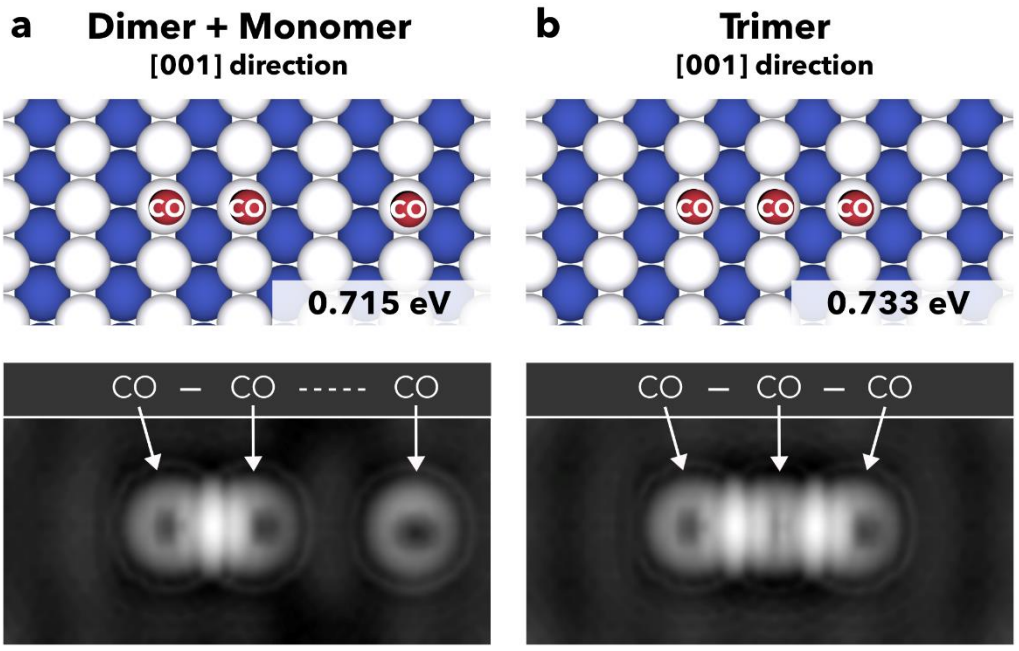

Fig. 4. Optimised geometries for three CO molecules in the same unit cell. (a) a dimer and a monomer, and (b) a trimer. White (blue) spheres represent the Cu atoms belonging to the first (second) layer of the substrate. Adsorption energies (in eV/per CO molecule) are shown at the bottom of each optimised structure. The bottom panels show the constant-current STM simulated images corresponding to the geometries shown in (a) and (b), respectively (iso-surface value $5 \cdot 10^{-4}$ e/Å^3, V_t = 0.2 V corresponding to empty states imaging).

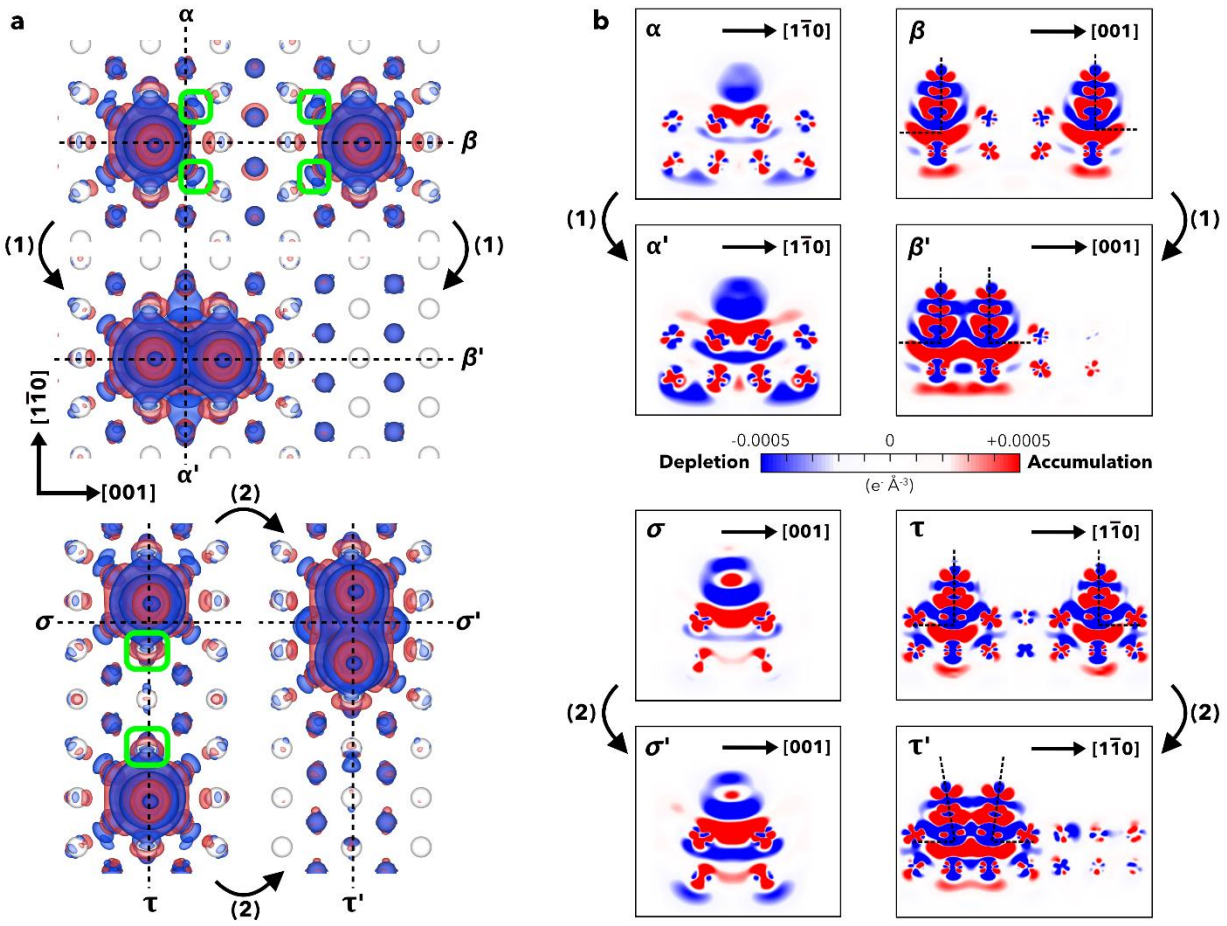

Fig. 5. (a) Computed adsorption-induced charge density difference maps showing the redistribution of charge on forming a dimer along the [001] (top panels) and the [1$\bar{1}$0] (bottom panels) substrate directions. Red and blue indicate an increase and a decrease, respectively, of electron density. (b) Cuts through the charge density difference plots in (a) along the normal planes indicated by Greek letters and dotted lines. Electronic iso-surfaces at $5 \cdot 10^{-4}$ electrons/Å^3.

Graphical Table of Contents: